



**HAL**  
open science

## Yb: YAG laser welding of aeronautical alloys

Joel Alexis, Jean Denis Beguin, Pablo Cerra, Yannick Balcaen

► **To cite this version:**

Joel Alexis, Jean Denis Beguin, Pablo Cerra, Yannick Balcaen. Yb: YAG laser welding of aeronautical alloys. Materials Science Forum, 2018, 941, pp.1099-1104. 10.4028/www.scientific.net/MSF.941.1099 . hal-02359734

**HAL Id: hal-02359734**

**<https://hal.science/hal-02359734v1>**

Submitted on 12 Nov 2019

**HAL** is a multi-disciplinary open access archive for the deposit and dissemination of scientific research documents, whether they are published or not. The documents may come from teaching and research institutions in France or abroad, or from public or private research centers.

L'archive ouverte pluridisciplinaire **HAL**, est destinée au dépôt et à la diffusion de documents scientifiques de niveau recherche, publiés ou non, émanant des établissements d'enseignement et de recherche français ou étrangers, des laboratoires publics ou privés.



## Open Archive Toulouse Archive Ouverte




OATAO is an open access repository that collects the work of Toulouse researchers and makes it freely available over the web where possible

This is an author's version published in: <http://oatao.univ-toulouse.fr/22803>

### Official URL:

<https://www.scientific.net/MSF.941.1099>

### To cite this version:

Alexis, Joel  and Beguin, Jean Denis  and Cerra, Pablo and Balcaen, Yannick  *Yb: YAG laser welding of aeronautical alloys*. (2018) Materials Science Forum, 941. 1099-1104. ISSN 1662-9752

Any correspondence concerning this service should be sent to the repository administrator: [tech-oatao@listes-diff.inp-toulouse.fr](mailto:tech-oatao@listes-diff.inp-toulouse.fr)

# Yb: YAG Laser Welding of Aeronautical Alloys

Joel Alexis<sup>1,a\*</sup>, Jean-Denis Beguin<sup>1,b</sup>, Pablo Cerra<sup>1,c</sup>, and Yannick Balcaen<sup>1,d</sup>

<sup>1</sup>Laboratoire Génie de Production, LGP, Université de Toulouse, INP-ENIT, Tarbes, France

<sup>a</sup>joel.alexis@enit.fr, <sup>b</sup>jean-denis.beguin@enit.fr, <sup>c</sup>pcerra@enit.fr, <sup>d</sup>yannick.balcaen@enit.fr

**Keywords:** laser welding, titanium alloy, aluminium alloy, superalloys.

**Abstract.** Interest in the use of laser technology is growing in the aeronautical sector. The implementation of new Yb: YAG solid laser sources and new optical generations (dynamic focal length; 2in1 fiber: Fiber core and ring core) offers advantages in terms of quality, accuracy, reproducibility and weld dimensions. The LASER beam Yb: YAG of these new sources is generated, no longer from a bar of yttrium-aluminum garnet but from a disk. Moreover, a top-hat shaped power distribution and a top-hat shaped power distribution with a sharply limited recess in the center (ring structure) may be at the focal point using respectively the inner fiber and the coaxial fiber. These technological innovations offer new possibilities for cutting and welding of sheet metal parts. The welding domains of EN AW-6061 aluminum alloy, Commercial Purity Titanium - Grade 2 (T40), AISI 321 stainless steel alloy, nickel based Hastelloy X and Inconel 625 and cobalt based Haynes 188 superalloys are defined according to process parameters such as power density, focal diameter, welding speed and fiber type. Optimal welding parameters are determined for each alloy. The evolution of the microstructures and the mechanical properties of each zone of the welds are explained according to the power density, the heat input energy and the welding speed.

## Introduction

The fuselage parts of an aircraft are historically assembled by riveting. In recent years, much research has been conducted into the replacement of the riveting process by friction stir welding or laser welding techniques [1]. The laser welding process has been a mature process in the automotive industry. Its implementation in the aviation industry is still minor despite its many benefits. Gialos *et al.* shows that the laser welding process compared to the riveting process for the manufacture of stiffened panels, would allow a time saving of 67%, a labor saving of up to 32%, a global manufacturing savings 40% [2]. For example, the lower fuselage panels of the A318, A340-600 and A380 are no longer riveted but welded. In addition, many developments in laser sources and laser beam transport systems have emerged in recent years. Nowadays, Disk lasers have higher power, higher efficiency and higher optical quality compared to older CO<sub>2</sub> laser sources [3-4]. The Nd: YAG, Yb-fiber and Yb: YAG discs lasers have a wavelength of about 1 μm and can therefore be transmitted on optical fibers several tens of meters in length to the focusing optics. In addition, they can be switched between different distribution fibers giving more flexibility to the production. In comparison, the CO<sub>2</sub> laser sources have a wavelength of about 10 microns that cannot be focused by optical fibers, and therefore must be directed to the workpiece using a series of lenses. The objective of this paper is to determine the domain of weldability by laser disk welding process of several aeronautical alloys: an aluminum based, a commercially pure titanium, a stainless steel, two nickel based superalloys and a cobalt base superalloy. Weld dimensions, microstructure and mechanical properties are discussed in terms of welding parameters and materials.

## Experimental Methods

The alloys studied are: EN AW-6061 aluminum alloy, CP Ti grade 2 titanium alloy, AISI 321 stainless steel, and Inconel 625, Hastelloy X, and Haynes 188 superalloy. The metallurgical state of the sheets, their mechanical and physical properties are given in Table 1.

Table 1. Metallurgical state and mechanicals properties of the alloys.

Alloys	Heat treatment	Thickness t (mm)	UTS [MPa]	YS [MPa]	Elongation [%]*	Melting range [°C] *	Thermal conductivity [W.m <sup>-1</sup> .K <sup>-1</sup> ]*
<b>AISI 321</b>	Annealed	1.2	620	240	45	1400 - 1425	16.1
<b>Inconel 625</b>	Annealed	1.2	940	460	50	1290 - 1350	9.8
<b>Hastelloy X</b>	Annealed	1.2	795	415	58	1260 - 1355	9.2
<b>Haynes 188</b>	Annealed	1.2	1005	495	68	1315 - 1410	10.4
<b>CP-Ti Gr2</b>	Annealed	0.8	430	340	28	1665	16.4
<b>EN AW-6061</b>	T4	1	240	145	22	582 - 652	154.0

\* : from ASM specification [5]

The samples were cut and butt welded with TRUMPH TruLaser Cell 3000 machine. The laser beam is generated by a Yb: YAG TruDisk source, with a maximum continuous power of 3 kilowatts, equipped with a special optical fiber comprising a 100  $\mu\text{m}$  core fiber and 400  $\mu\text{m}$  coaxial fiber. To identify influential parameters of the welding process while streamlining testing, an experimental design was established with the CORICO® software [6] to understand the new possibilities offered by this new technology. The laser power, the speed welding, the focal diameter and the gas flow were the parameters studied (Table 2).

Table 2. Design matrix defined by the CORICO® software.

	Power [W]	Speed [m.min <sup>-1</sup> ]	$\varnothing_{SF}$ [ $\mu\text{m}$ ]	$\varnothing_{LF}$ [ $\mu\text{m}$ ]	Gas flow [L.mn <sup>-1</sup> ]
S1	1000	6.25	305	375	25
S2	1500	1.00	120	480	10
S3	2500	8.00	175	525	40
S4	2500	4.50	240	600	32
S5	1500	8.00	240	600	32
S6	1000	6.25	175	525	25
S7	1500	1.00	305	675	32
S8	2000	6.25	175	525	17
S9	2000	8.00	305	675	17
S10	2000	2.75	305	675	40
S11	1000	6.25	240	600	32
S12	2000	4.50	305	675	10
S13	2000	6.25	370	750	40
S14	1500	4.50	370	750	17
S15	1000	2.75	240	600	32
S16	2500	2.75	270	750	17
S17	1500	6.25	120	480	40
S18	500	2.75	175	525	25
S19	2500	1.00	240	600	25
S20	500	4.50	205	675	10
S21	1000	4.50	370	750	17
S22	500	8.00	120	480	25
S23	2000	2.75	175	525	32
S24	1500	4.50	240	600	25
S25	500	8.00	120	480	10
S26	500	1.00	370	750	10
S27	500	1.00	120	480	40
S28	2500	1.00	120	480	10
S29	2500	8.00	370	750	40
S30	500	1.00	120	480	10

The laser beam can be carried by the core of the fiber; the focal diameter is considered small (SFC). It can also be carried by the periphery of the fiber, which then corresponds to the large focal configuration (LFC) [7-8]. To validate the weldability of these alloys, dimensions of weld section are measured and compared to standard specifications described in NF L06-395-2000. The welds are observed in section by optical microscopy after metallographic preparation. The mechanical properties of the welds are determined by tensile tests, carried out with a crosshead speed of  $2 \text{ mm} \cdot \text{min}^{-1}$ . After testing, the rupture zone is identified by optical microscopy or scanning electron microscopy.

## Results and Discussion

### Welding windows: influence of welding parameters on the achievement of full penetration welds.

Weldability domains are represented on figure 1, for both core (fig. 1a) and outer fiber (fig.1b), and for previously listed materials. To represent the results of this three parameters experiment matrix, these domains are plotted on an interaction time  $\tau$  – calculated as the focus diameter divided by the welding speed – vs. power density  $I$  diagram. Light gray dots represent the experimental matrix.

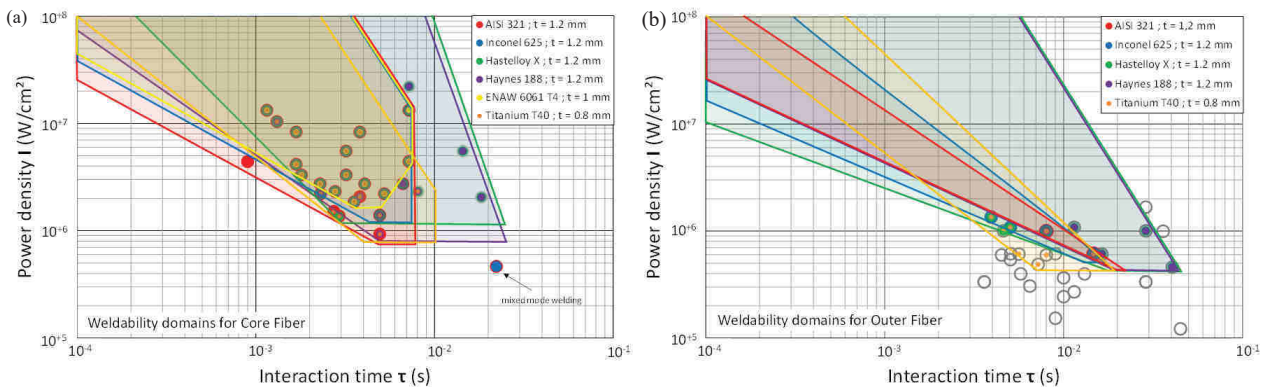


Figure 1. Weldability domains of selected alloys, for core fiber (a), and outer fiber (b).

Analysis of the weldability domain with core fiber reveals several information. First, considering that for most materials, it can be assumed that the keyhole welding mode is triggered for power density above  $10^6 \text{ W} \cdot \text{cm}^{-2}$  [9], most of the weld achieved with core fiber seems to be in keyhole welding mode. It can explain the easy achieving of full penetration welds for most materials, excepting AW-6061 aluminum alloy, known to present high thermal conductivity, and high optical reflectivity [10]. The second point is that the upper bound of interaction time seems to be related to both thickness and thermal conductivity (table 1). The higher the thermal conductivity, the higher the upper bound of interaction time. This assertion will be discussed in the next part of this paper.

Concerning outer fiber welding domains, it can be observed that these are more restrictive than the core fiber ones. The upper and lower bound of the welding domains are respectively  $1.5 \cdot 10^6$  and  $4 \cdot 10^5 \text{ W} \cdot \text{cm}^{-2}$ . Lower power densities produce shallow weld beads, with weak penetration, regardless the interaction time. Another bound of these domains is given by the fluence  $F$ , calculated as  $I \times \tau$ , and expressed in  $\text{J} \cdot \text{cm}^{-2}$ . High levels of fluence can lead to weld pool instabilities, and finally cut-through phenomenon. For example, the upper limit of fluence for T40, AISI 321 and Inconel 625 is near  $10^4 \text{ J} \cdot \text{cm}^{-2}$  and could be  $3 \cdot 10^4 \text{ J} \cdot \text{mm}^{-2}$  for Hastelloy X and Haynes 188. About aluminum, catastrophic hot cracking, incomplete penetration or complete cut-through phenomena did not permit to obtain any sound welds.

### Influence of Process Parameters on Weld Bead Geometry.

To understand the relationship between process parameters and weld bead geometry, an interaction time vs. weld bead width representation is proposed on figure 2. It has been determined that, within the different welding domains, the interaction time was the most pertinent process parameter to describe geometric evolutions of weld beads.

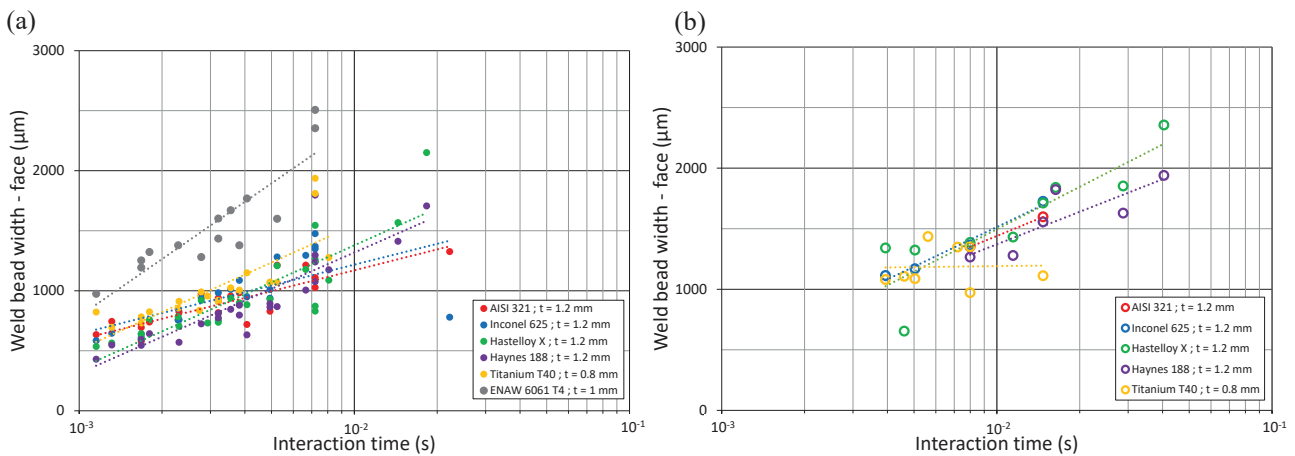


Figure 2. Evolution of the face weld bead width versus interaction time, for full penetration welds, using core fiber (a), and outer fiber (b).

It can be observed that the weld bead width seems positively related to the interaction time, but this behavior could be largely influenced by material properties. The upper limit of interaction time on these alloys can be related to the maximal width of the weld tolerated before weld pool collapse. AW-6061 aluminum alloy is highly sensitive to this parameter and produces wide weld. It has been highlighted in the previous part that the welding domain of this alloy was the narrowest of the tested materials, limited by weld pool collapse at high interaction time. This is due to its high thermal conductivity and low melting temperature. All other materials, exhibiting ten times lower thermal conductivities, and higher melting temperatures, presented lower sensitivity to this phenomenon.

### Influence of Weld Beads width upon Mechanical Properties of Assemblies.

After proposing a relation between a chosen process parameter and geometric features, a link is suggested between the latter and ultimate tensile test of obtained assemblies on figure 3.

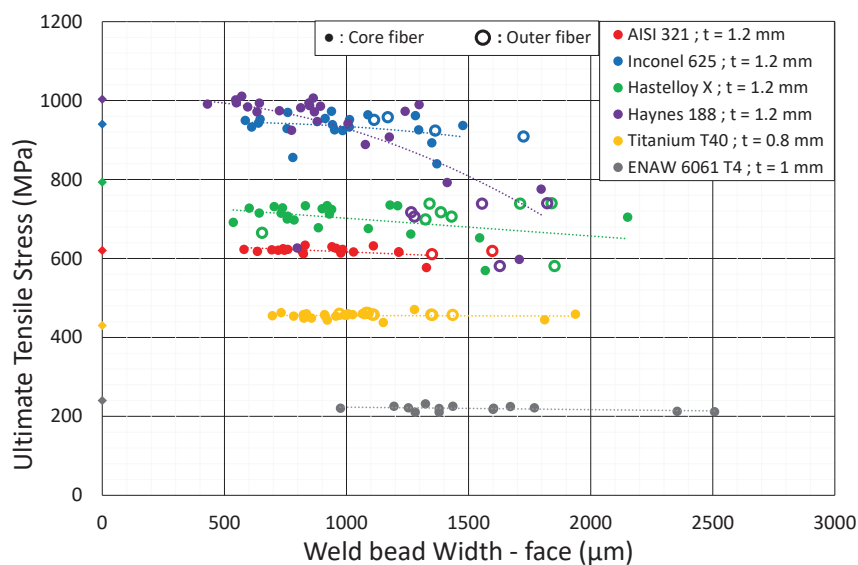


Figure 3. Evolution of Ultimate Tensile Stress versus weld bead width for full penetration welds of selected materials.

Concerning aluminum alloy, a weak but constant deterioration of UTS is evidenced. Tensile test revealed that fracture is systematically localized in Fusion Zone (FZ), but after a noticeable plastic

deformation (between 7 and 12 % of total strain), in the vicinity of the strain hardening plateau occurring near UTS of the base metal. The microstructures of fusion zones consist in fine dendritic grains surrounded by silicon enriched interdendritic areas, with potential depletion of magnesium due to vaporization. These microstructures can explain the lower properties of the fusion zone compared to the base metal. Onward studies will deal with effects of post-welding heat treatments on mechanical properties of these assemblies.

About commercial purity titanium T40, tested sample fractured in base metal, far from the fusion zone excepted for the wider weld bead (sample S30). The fine acicular microstructures within the FZ can explain this behavior, even though Heat Affected Zones (HAZ) present grain coarsening phenomenon.

Austenitic alloys exhibit various behavior. Mechanical properties of nickel and cobalt based alloys are clearly dependent to the width of the weld bead, especially Haynes 188. Generally, for all these alloys, fracture occurs in FZ. Microstructures of these FZ consist in fine cellular structure epitaxial grown from the base metal, to fine dendritic grain structure in the centerline of the weld (Fig. 4) [11]. Concerning mechanical properties, it appears that the wider is the weld, the most the UTS of the assembly is affected.

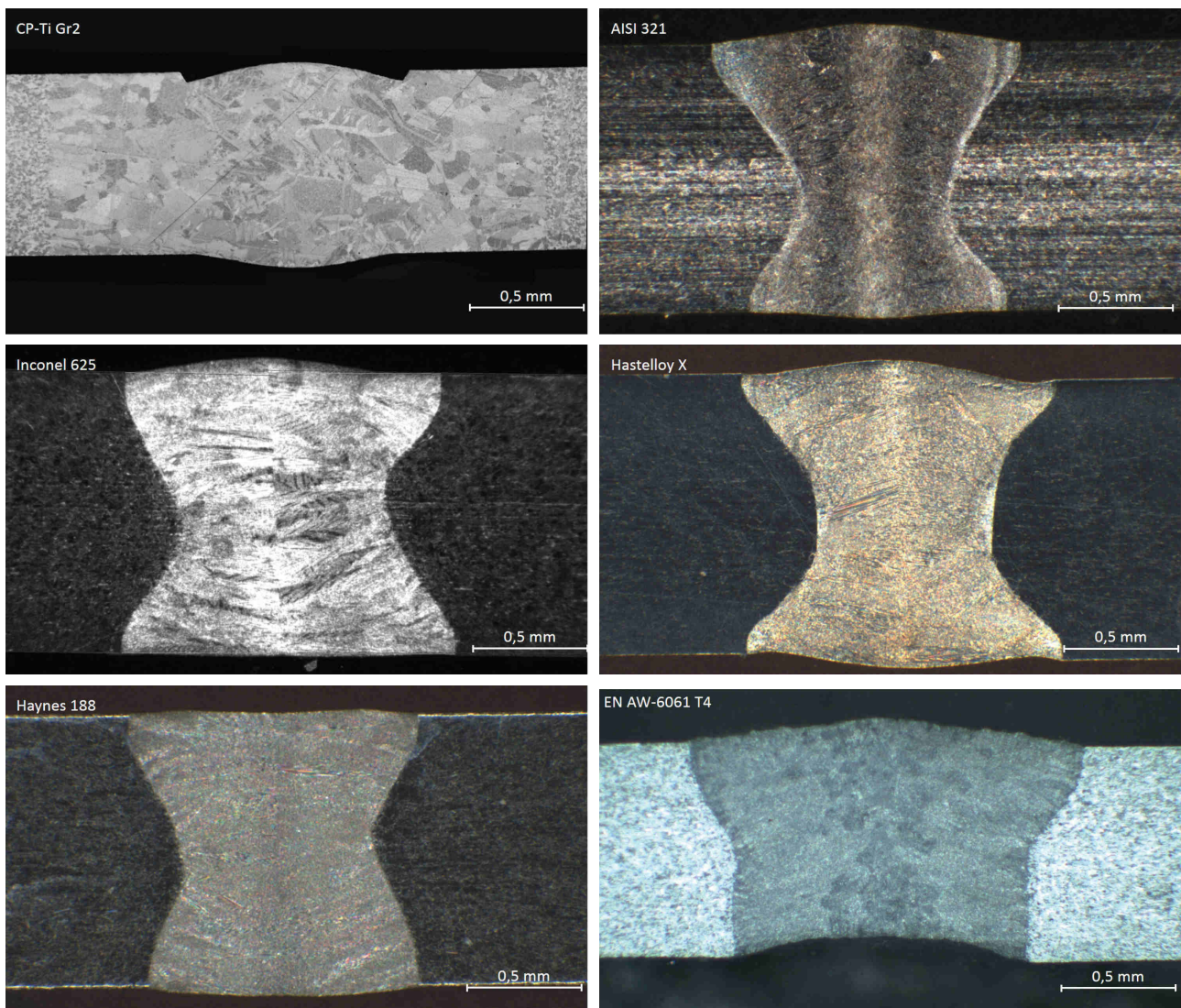


Figure 4. Optical macrographs of welded samples using S4 process parameters (Outer fiber welding for all alloys except for AW 6061, welded using core fiber).

Hastelloy X and Haynes 188 welds presented also an important feature: the amount of  $M_6C$  carbides, estimated by transmission X-ray diffraction, seems to be sharply decreased in the FZ [11]. This is the draft of an explanation of the lower properties of these assembly.

AISI321 appears less sensitive to this phenomenon, because of the nature of its hardening mechanism based on chromium and nickel solid solution only.

## Conclusion

Concerning effect of the outer core fiber use and its possible advantages in welding process, they could be, on one hand, the ease of obtaining weld beads near free of geometric defects such as undercut, underfill or excessive reinforcement. On the other hand, for larger weld bead width than ones obtained by core fiber, some outer fiber welded samples of AISI 321, Inconel 625 and Hastelloy X can present similar UTS values.

The main drawbacks are, on one side the difficulty to achieve full penetration on 1.2 mm thick sheets of AISI 321 and Inconel 625 alloys (small welding domain), and on the other side its inability to obtain sound welds on ENAW 6061 aluminum alloy.

## References

- [1] M.C. Chattervedi, (Ed.), *Welding and joining of aerospace materials*, Woodhead Publishing in materials. Woodhead Publishing, Cambridge, UK : Philadelphia, PA. 2012.
- [2] A.A. Gialos, V. Zeimpekis, N.D. Alexopoulos, N. Kashaev, S. Riekehr, and A. Karanika, Investigating the impact of sustainability in the production of aeronautical subscale components. *J. Clean. Prod.* 176, (2018) 785–799.
- [3] A.Giesen, and Speiser J., Fifteen Years of Work on Thin-Disk Lasers: Results and Scaling Laws. *IEEE J. Sel. Top. Quantum Electron.* 13, (2007) 598–609.
- [4] G. Verhaeghe, and B. Dance, ‘An assessment of the welding performance of high-brightness lasers and a comparison with in-vacuum electron beams’.*Proc. Int. Conf of Appl. of Lasers and Electro-Opt.*, ICALEO, Temecula, USA, (2008) 406–414.
- [5] ASM website : <http://www.aerospacemetals.com/index.html>
- [6] M. Lesty, Une nouvelle approche dans le choix des régresseurs de la régression multiple en présence d'interactions et de colinéarités. *La revue de Modulad* 22 (1999) 39-77.
- [7] J. Graneix, J.-D. Beguin, J. Alexis, and T. Masri, Influence of Yb: YAG Laser Beam Parameters on Haynes 188 Weld Fusion Zone Microstructure and Mechanical Properties. *Metall. Mater. Trans. B* 48, (2017).
- [8] J.Graneix, J.-D. Beguin, F. Pardheillan, J. Alexis, and T. Masri, Weldability of the superalloys Haynes 188 and Hastelloy X by Nd:YAG. *MATEC Web Conf.* 14, (2014) 13006.
- [9] L. Quintino, E. Assunção, Conduction laser welding, *Handbook of Laser Welding Technologies*, Woodhead Publishing Cambridge, UK: Philadelphia, PA. (2013) 139-162
- [10] J. F. Ready, *Industrial applications of Lasers*, Academic press, New York (1997)
- [11] Graneix, J. Étude du soudage laser Yb: YAG homogène et hétérogène des superalliages Hastelloy X et Haynes 188, thesis Université de Toulouse (2015)